A Theory of the Effective Yield Stress of Foam in Porous Media: the motion of a soap film traversing a three-dimensional pore

S.J. Cox [a,*] S. Neethling [b] W.R. Rossen [c] W. Schleifenbaum [a,1]
P. Schmidt-Wellenburg [a,2] J.J. Cilliers [b]

[a] *Department of Physics, Trinity College, Dublin 2, Ireland*

[b] *Chemical Engineering, UMIST, P.O. Box 88, Manchester M60 1QD, UK*

[c] *Department of Petroleum and Geosystems Engineering, The University of Texas at Austin, 1 University Station C0300, Austin, TX 78712-1061, USA.*

Abstract

The effective yield stress of foam in porous media depends on the capillary resistance of the soap films between bubbles, or lamellae, to forward movement. This resistance depends in turn on the shapes lamellae take as they move across pores. Even in idealized, radially symmetric pores, lamellae spontaneously jump to asymmetric shapes in their drive to minimize their surface area. These shapes affect the overall capillary resistance to foam movement. Earlier theoretical study of quasi-static lamella movement in two dimensions (2D) is extended here to three dimensions (3D) using the Surface Evolver computer program. Whereas in 2D the lamella can take flat, asymmetric shapes in the pore body, in 3D it can take a sequence of saddle-shapes of increasingly negative mean curvature as the trailing edge of the lamella approaches the middle of the pore. The results based on 2D lamellae are altered in detail but not in essence: the asymmetric jump increases the capillary resistance to foam movement, and for small bubbles in small pores the minimum pressure gradient required to drive gas flow in foam is substantial.

Key words: Foam, Porous Media, Minimal Surfaces, Yield stress, Surface Evolver

* Corresponding author.
Email address: simon.cox@tcd.ie (S.J. Cox).
[1] Permanent address: Fachbereich Physik, Technische Universität Darmstadt, Germany
[2] Permanent address: Fachbereich Physik, Technische Universität München, Germany

1 Introduction

Foams are used worldwide in the petroleum industry for diverting acid flow in well stimulation [1], and on a pilot basis for gas diversion in improved-oil-recovery processes [2, 3] and environmental remediation [4]. In all these cases, when the foam enters the porous medium, the bubbles in the foam are thought to be as large as, or larger than, the pores in the medium [3, 5]. Moreover, most of the gas in the foam is trapped [6, 7], so that the bubbles that do flow move in "bubble trains" through pore pathways in the midst of trapped gas [8], as schematically illustrated in Fig. 1.

Developing a fully mechanistic and predictive model for foam [8, 10, 11] requires an understanding of how foam of a given average bubble size affects gas mobility in the porous medium. (Other components of the model would describe the processes that control bubble size.) In particular we focus here on the effective yield stress that foam imparts to the gas phase in porous media [10]. This yield stress arises from the resistance to forward movement of the soap films, or lamellae, that separate bubbles in the train. In the limit of zero velocity, this resistance arises from each lamella in the train trying to minimize its surface area, subject to conserving the volume of gas in each bubble and to the geometric constraints of the pore walls.

Rossen [12] addressed this problem by idealizing the pore walls between which the bubble train passes as a series of identical bi-conical pores with either sharp or rounded corners at the widest part of the pore body. The rounded shape is more realistic, even if the solid pore wall has a sharp corner at the pore body, because water would fill the sharp corner, in approximate capillary equilibrium with the surrounding medium [9, 13]. The pore-geometrical parameters based on this model are defined in Fig. 2. In the absence of contact-angle hysteresis, the lamella is everywhere perpendicular to the pore wall. The minimum pressure gradient required to advance a series of bubbles and lamellae as in Fig. 1 is the population-average pressure drop across the individual lamellae, multiplied by the number of lamellae per unit length in the direction of flow [12]. For incompressible foams, the population-average pressure drop per lamella in turn equals the time-averaged pressure drop Δp^{ave} for one lamella traversing one of the pores in steady volumetric flow [14]. In a fully mechanistic foam model one could either apply this minimum pressure gradient for flow directly or represent it as an effective yield stress for the gas phase in foam [10].

With an idealized pore geometry that is front-back and up-down symmetric (in 2D) or radially symmetric (in 3D), it is natural to assume that the lamella shapes would also show this same symmetry. Rossen [12]–[16] showed that this is untrue, in both 2D and 3D. The breaking of front-back symmetry in lamella movement across the pore (referred to hereafter as a symmetric jump) gives foam a nonzero yield stress, and the breaking of axial symmetry (an asymmetric jump) further increases the

yield stress. Rossen [14, 15] shows examples. Any experimental demonstration, however, must confront doubts about possible contamination of the solid surface, non-uniform wetting of the surface, slight asymmetries in the pore, etc. Rossen was unable to represent asymmetric lamella shapes analytically in 3D, and had to revert to 2D geometry in an analysis of lamella shapes that break axial symmetry.

In 2D the asymmetric jump increases the value of Δp^{ave} markedly. It is unclear whether the effect is as large in 3D, for several reasons. Firstly, in 2D the asymmetric shapes have zero curvature as the lamella straddles the pore body, which gives a sequence of shapes with zero Δp. In 2D the lamella contacts the pore wall at only two points; in 3D, as the lamella advances, its perimeter contacts more and more of the converging pore wall, and the requirement that it be perpendicular to this wall imposes more and more drive toward negative curvature. Therefore, the asymmetric jump may not raise Δp^{ave} as much in 3D as in 2D.

Rossen [16] reports rough measurements of lamella curvature in a sequence of positions as a lamella traversed a model glass pore of length about 10 cm. (Pore size was too large, and capillary Δp too small, to measure Δp directly in this experiment.) In this case there were also complications of interactions with other lamellae lodged in pore throats fabricated into the pore body. Rossen then compared his rough measurements with the corresponding pore modeled in 2D. The value of Δp^{ave} in 3D was about one-quarter of the estimate based on the 2D model; moreover, given the roughness of the measurements, the uncertainty in Δp^{ave} was nearly as large as its value. Thus there is uncertainty about the magnitude of Δp^{ave} and the role of the asymmetric jump in 3D.

Recently, the Surface Evolver computer program [17] has made it feasible to determine computationally the lamella shapes and pressure drops in complex situations that include volume constraints and the requirement that the lamella contact a solid surface such as a pore wall. Adapting the Surface Evolver to this problem requires some care, as discussed below. This paper describes calculations of lamella shapes in 3D pores, the time-average pressure drop across the 3D lamella, and the implications for effective yield stress of gas in foam flow through porous media.

We treat here the *quasi-static* problem, i.e. we assume that the motion is slow enough that (i) there are no gradients of surface tension, (ii) there is no viscous drag on the ends of the lamella, and (iii) there is no contant-angle hysteresis. The relaxation of these conditions leads to higher time-average pressure drops [9, 12, 13]. It is therefore appropriate to choose a contact angle of 90° between the lamella and the pore wall, and uniform surface tension for the lamella. The evolution of the lamella then proceeds by short increments, minimizing area at each step. The Surface Evolver then tells us which lamella has the lowest surface area among all possible lamellae that meet a given pore wall perpendicularly and enclose a given volume.

We shall consider two shapes for the pore body, each in two and three dimensions. In §2 we will motivate our work with reference to the two-dimensional bi-conical pore proposed by Rossen [12]. This provides a verification of the use of the Surface Evolver for this problem. In 3D it is not clear if the time-averaged pressure drop increases significantly for an asymmetric compared to a symmetric jump, as it does in 2D [16]. We therefore describe Surface Evolver simulations in §3 which have enabled us to visualize, for the first time, the lamella shapes and pressure differences across lamellae undergoing asymmetric jumps. We show that the average pressure drop is lower than in 2D, but still larger than for a symmetric jump. Finally we discuss the case of a sinusoidal pore in §4 which has a much smoother shape and correspondingly low average pressure drops. In each case we will consider the same dimensions of the pore, i.e. throat radius, body radius and length, presuming that these are representative of the behaviour of the lamella and the average pressure drop in a wide range of pore-shapes.

2 Bi-conical pore in two-dimensions

We start by considering the motion of a single lamella through a two-dimensional bi-conical, or wedge-shaped, pore, shown in Fig. 2(i). In two dimensions the lamella is always a circular arc that meets the pore wall perpendicularly, since it minimizes its surface energy (length in 2D). The pore is of length $2L$ and at its widest part has height (or radius) R_b. The throat region is of height $R_t = 0.2L$ and we introduce a rounded region at the centre of the pore body of width $2\epsilon L$. In the rounded region the pore wall is defined by a parabola that smoothly fits the slope of the pore wall on both sides of this region. The shape of the pore wall is therefore given by

$$r_c(x) = \begin{cases} R_t + (R_b - R_t)\dfrac{x}{L} & 0 \le x \le L(1-\epsilon) \\ R_b - \dfrac{\epsilon}{2}(R_b - R_t) - \dfrac{R_b - R_t}{2\epsilon L^2}(x-L)^2 & L(1-\epsilon) \le x \le L(1+\epsilon) \\ 2R_b - R_t - (R_b - R_t)\dfrac{x}{L} & L(1+\epsilon) \le x \le 2L. \end{cases} \quad (1)$$

In 2D, $r_c(x)$ represents the distance of the pore wall from the x-axis – it is reflected in the $x-$axis to define the body of the pore. This notation, and pore shape, will also be used later for a radially symmetric 3D pore, with r_c corresponding to its radial distance from the axis of rotation. In what follows we use parameter values of $R_b = L$ (pore diameter equal to pore length), $R_t = 0.2L$ and $\epsilon = 0.05$.

The pressure drop across a lamella is $\Delta p = 2\sigma/R$, where σ is surface tension and R is the radius (of curvature) of the lamella. This is non-dimensionalized by dividing by the capillary entry pressure of the pore throat in 2D:

$$\Delta p_D = \Delta p/(2\sigma/R_t). \quad (2)$$

Then the time-averaged pressure drop is

$$\Delta p_D^{\text{ave}} = \int_0^1 \Delta p_D \mathrm{d}(\mathrm{V_D}). \tag{3}$$

Here the dimensionless volume V_D is the volume behind the lamella divided by the total volume of the pore. With a steady volumetric injection rate, this variable also represents dimensionless time.

Lamella shapes are known analytically in 2D, and there are stability criteria to predict when the lamella makes asymmetric jumps [9, 15]. Thus the 2D case provides a test of the accuracy of the Surface Evolver calculations before we tackle the 3D case, where for some of the lamella shapes there are no checks on the Surface Evolver results.

2.1 Symmetric jump

Since the idealized pore is up-down symmetric, one might assume that the lamella is also symmetric. Rossen [12] first made this assumption in his analysis of 3D pores. Fig. 3(i) shows schematically the sequence of lamella shapes, where for simplicity we have left out the rounded region at the pore body ($\epsilon = 0$). In this case it is straight-forward to calculate the sequence of lamella shapes, the volume behind the lamella, and the pressure drop across the lamella as in Figs. 4 and 5.

Fig. 4 shows how the volume behind the lamella changes with the positions of attachment, x_1 and x_2, of the lamella to the pore wall. For small ϵ, the volume goes through a maximum as the lamella enters the rounded region at the pore body ($x_1/L = x_2/L = 1 - \epsilon$), with $V_D = 0.643$ in the case $\epsilon = 0.05$. At this point the lamella has spent about 64% of its time in the pore with a positive curvature (bulging forward), i.e. resisting forward movement. Continuous forward movement of the lamella from this point is impossible without violating the volume constraint on the rearward bubble; therefore the lamella jumps forward, from $x/L = 0.950$, to a position $x/L = 1.348$ with the same volume as before the jump. The lamella now bulges backwards with negative curvature. Thus the front-back symmetry of the boundary conditions (pore wall) is broken in the movement of the lamella. From this point forward lamella shape is the mirror image of that when the lamella entered the pore.

Fig. 5 shows how the pressure drop across the lamella changes during this process, referring for the moment only to the analytical result. Initially the lamella is flat (shape **a** in the pore throat ($x = 0$)). Then it rapidly bulges forward to its shape of maximum positive curvature (**b**) before it leaves the throat. The pressure difference across the lamella decreases as the radius of the lamella increases, until the

lamella jumps (from point **c** at the pore body). From this point forward the curvature bulges backwards and the pressure drop is negative. Surface tension here pulls the lamella forward into the throat just as it resisted forward movement from the preceding throat. The dotted line in Fig. 5 shows the pressure difference that would be observed if the lamella reversed direction after its jump.

For the case $\epsilon = 0$, Rossen [12] showed that the time-averaged pressure drop is

$$\Delta p_D^{\text{ave}} = 0.120 \quad \text{2D bi-conical pore; symmetric jump; } \epsilon = 0$$

with this value decreasing as ϵ increases: the increasing roundness of the pore wall makes the jump less severe. For ϵ greater than about 0.25, there is no maximum in the volume and we therefore expect no symmetric jump.

2.2 Numerical procedure

We used the Surface Evolver [17] in this 2D case to verify that we find the same lamella shape and pressure drop, as a function of volume, as the analytical values. In its basic mode of operation, this software finds the minimum-energy configuration of a system for the given topology, subject to volume and boundary constraints. It requires a set of vertices to be defined, which are then joined by (oriented) edges. An ordered loop of edges defines, in 2D, a bubble. Each of the edges may be discretized into small elements, and then each of these can be moved to determine the shape of minimum energy.

We therefore define two constraints which correspond to the upper and lower edges of the pore body according to (1) and define edges that lie on these constraints. A single edge, the lamella, is defined to connect them with tension 1, and the pore throats at each end of the body are capped by fixed straight lines of zero tension. The region to the left of the lamella is defined to be a bubble of given volume V; the region to the right has zero pressure, so that the pressure associated with the bubble is also the required pressure difference Δp.

We commence the quasi-static evolution of the lamella by first ensuring that the discretization is accurate enough to capture the shape of the curved region at the apex of the pore body, using about four levels of refinement (in 2D, each refinement step corresponds to halving the length of each edge) and "quadratic" mode (each edge is parabolic rather than straight) which corresponds in this case to about 80 edge segments. We then increase the volume of the bubble by a small amount, $\delta V \approx 0.01V$, and iterate many times until the lamella reaches its new minimal shape. Current volume, pressure difference and the point of contact between the lamella and the pore boundary are then recorded, and the process repeated. The resulting pressure-volume data are shown in Fig. 5, indicating that the agreement

of the Evolver results with the analysis is excellent.

We are also able to calculate the time-averaged pressure drop using a trapezoid-rule calculation which involves adding the bubble's pressure at each point in the evolution. For $\epsilon = 0.05$ we find

$$\Delta p_D^{\text{ave}} = 0.0853 \quad \text{2D bi-conical pore; symmetric jump; } \epsilon = 0.05$$

which agrees precisely with the analytic calculations (Table 1). This is significantly less than the result for $\epsilon = 0$, and decreases further with increasing ϵ. Thus, the rounder the pore boundary, the lower the average pressure drop.

2.3 Asymmetric jump

Even in perfectly radially symmetric pores, however, lamellae spontaneously make asymmetric jumps, as shown by Rossen [12]. The case for a pore with a sharp corner, $\epsilon = 0$, is shown schematically in Fig. 3(ii). Given the volume constraint on the bubble behind the lamella, the positions of attachment of the two ends of the lamella to the pore walls, x_1 and x_2, determine lamella shape. In 2D, lamella surface energy is then a function of x_1 and x_2. As the lamella approaches the pore body, the Hessian of energy with respect to x_1 and x_2 becomes singular. Moreover, the eigenvector corresponding to the zero eigenvalue indicates that one side of the lamella moves forward and one back in an unstable perturbation. The lamella therefore jumps to an asymmetric, flat shape (**e** in Fig. 3(ii)) with zero pressure difference, as shown in Fig. 5. It retains this shape as it advances, until its trailing edge approaches the apex of the pore body (shape **f**), at which point it jumps back to a symmetric shape with negative curvature for the remainder of its passage through the pore. In Fig. 4 the split in the path corresponds to the jump to the asymmetric shape, with $x_1 \neq x_2$.

Fig. 5 shows the consequences for the dimensionless pressure difference Δp_D. The jump to the asymmetric shape replaces part of the sequence of symmetric shapes with negative curvature, and therefore increases the value of Δp_D^{ave}. For the case shown, we find

$$\Delta p_D^{\text{ave}} = 0.178 \quad \text{2D bi-conical pore; asymmetric jump; } \epsilon = 0.05.$$

As ϵ decreases, the value of Δp_D^{ave} increases – it is equal to 0.217 for $\epsilon = 0$ [15].

The Surface Evolver simulations show the same asymmetric jumps. In other words, the algorithms in the Surface Evolver, seeking to minimize surface area, find the same asymmetric shapes taken by a lamella seeking to minimize its surface area

[9, 15, 16]. Examples are shown in Figs. 4 and 5. If, however, the volume increment δV is too large, then, rather than the asymmetric jump, the Evolver simulations show the symmetric jump. That is, if δV is of the order of the volume of the rounded region, the program may converge on a symmetric shape on the other side of the pore body (this is how the Surface Evolver models the symmetric jumps discussed in the preceding section). This is similar to the finding of Xu and Rossen [9] regarding lamella jumps at finite velocity in 2D. If the lamella is moving fast enough, it may clear the pore body and converge on a symmetric shape across the pore body before perturbations away from the symmetric shape have time to grow and push the lamella toward converging on an asymmetric shape. An animation of bubble movements in 2D, including quasi-static movement, is available at `http://www.cpge.utexas.edu/foam/`.

3 Bi-conical pore in three dimensions

We now consider the motion of a lamella through a bi-conical pore in three dimensions. We use (1) to describe the radially symmetric pore wall. In this case, when a lamella is also radially symmetric it takes the shape of a spherical cap, perpendicular to the pore wall. The pressure drop across a lamella is $4\sigma/R$, where R is the radius (of curvature) of the spherical lamella. The dimensionless pressure drop is now

$$\Delta p_D = \Delta p/(4\sigma/R_t) \tag{4}$$

while the time-averaged pressure drop is given by (3) as before.

In 3D we have analytical results for comparison while the lamella remains symmetric (i.e. spherical), but no analytical results for asymmetric shapes.

3.1 Symmetric jump

If the lamella remains symmetric, the sequence of shapes is analogous to that in 2D. The lamella flips to the rearward-facing spherical cap at $x/L = 1 - \epsilon$, where $V_D = 0.637$ for $\epsilon = 0.05$. Fig. 6 shows how the volume behind the lamella varies as it moves along the pore. The lamella shapes and the formulae relating volume, pressure difference and position of attachment are all analytic in the symmetric case, and the Evolver simulations show excellent agreement with these analytical results.

The pressure difference across the lamella is shown in Fig. 7 and the time-averaged

pressure drop in this case is

$$\Delta p_D^{\text{ave}} = 0.0793 \quad \text{3D bi-conical pore; symmetric jump; } \epsilon = 0.05.$$

compared to 0.126 in the case $\epsilon = 0$ [12]. Thus, after starting from a higher value at $\epsilon = 0$, the value of Δp_D^{ave} decreases more quickly, as ϵ increases, in 3D than in 2D for the symmetric jump.

3.2 Asymmetric jump

To calculate the pressure drop for the asymmetric jump, it becomes absolutely necessary to use the Surface Evolver, since determining the asymmetric shape of the lamella is a rather intractable mathematical problem. Since the simulations agree well for the 2D results and the 3D symmetric jump, we are confident that the Evolver should accurately predict the motion of a lamella in a 3D pore.

In 3D an oriented edge loop defines a face, which the Evolver immediately discretizes into triangular facets. A body is then made up of several faces, which can themselves be refined. There are, however, complications in using the same Evolver methodology in 3D as in 2D. The most serious of these is that the vertices defining the (initially circular) intersection of the lamella with the wall can shortcut the pore-wall constraint by sliding around the wall and "bunching-up", since this reduces the energy (area) of the lamella. We therefore define the constraint to be "convex", which introduces a penalty function to prevent this bunching, but also prevents the use of the Hessian facility which aids in determining stability. We also use "vertex averaging" which keeps the vertices well-spaced but increases the number of iterations necessary for convergence.

There is a further small but unavoidable error in that the Surface Evolver minimizes the area of the triangular elements, but the elements do not exactly represent the (curved) surface of the pore. Therefore there is a small error in both computed lamella area and bubble volume. This error shrinks as the refinement of the surfaces is increased.

In fact, we find that it is not possible to determine when the calculation has fully converged. In order to get an accurate estimate of the shape of the lamella in comparison with analytic calculations, we used of the order of 10^5 iterations for each increment in V, as well as the necessary tidying of the tessellation (removing small triangles, refining large ones, etc.). As before, we use approximately four levels of refinement (a refinement step partitions each triangular facet into four smaller ones) i.e. roughly 256 triangular, parabolically curved, faces to represent the lamella.

Notwithstanding these difficulties, we find good agreement in the data for the sym-

metric 3D jump, shown in Figs. 6 and 7. Our calculations for the asymmetric jump show that it occurs when $V_D = 0.637$, that is, when the trailing edge of the lamella meets the curved region of the pore wall (Fig. 6), as for the symmetric jump. After jumping, the shape of the lamella in 3D is a saddle – see Fig. 8. As it moves farther into the pore, the mean curvature (which is proportional to the pressure difference) of the saddle becomes increasingly negative, leading to more strongly curved shapes, as Rossen conjectured [16]. A qualitative comparison between Rossen's experiments [15] and the lamella shapes found here is shown in Fig. 8.

The pressure data for the asymmetric jump is shown in Fig. 7, where it is compared with the curve for the symmetric jump in 3D. The asymmetric jump occurs at the same volume V_D as the symmetric jump, at the beginning of the curved region. In the asymmetric case, however, the pressure doesn't immediately drop as low, thereby increasing the time-averaged pressure drop, which in this case is

$$\Delta p_D^{\text{ave}} = 0.104 \quad \text{3D bi-conical pore; asymmetric jump; } \epsilon = 0.05.$$

To enable further comparison with the 2D results, we wish to calculate the time-averaged pressure drop for an asymmetric jump in a bi-conical pore with $\epsilon = 0$, that is, a sharp corner. To estimate this, we performed a simulation with $\epsilon = 0.025$ (half the value used previously). The value of the pressure at each point in the evolution of the lamella during the asymmetric phase is virtually indistinguishable from the values for the higher value of ϵ and the lamella jumps back to the symmetric shape at the same position, shown in Fig. 9. Moreover, the volume of the pore remains constant up to order ϵ^2. Therefore the only significant difference is the delay in the jump occurring. So in the case $\epsilon = 0$ we can estimate the pressure drop by assuming that an asymmetric jump occurs at $x = L$, where $V_D = 0.721$, and hence calculate the time-averaged pressure drop. We find

$$\Delta p_D^{\text{ave}} = 0.138 \quad \text{3D bi-conical pore; asymmetric jump; } \epsilon = 0.$$

This is a relatively small increase on the value for $\epsilon = 0.05$ ($\Delta p_D^{\text{ave}} = 0.104$) and also only a small increase on the value for the symmetric jump in 3D with $\epsilon = 0.05 (\Delta p_D^{\text{ave}} = 0.126)$. Contrast this with the large difference in the average pressure drop between symmetric and asymmetric jumps in the 2D bi-conical pore – the latter is almost twice the former. We therefore find that, except for a symmetric jump with $\epsilon = 0$, the dimensionless average pressure drops are lower in three dimensions in each case. This is particularly marked for the asymmetric jumps, although the values of Δp_D^{ave} are still significant.

4 Sinusoidal pore

We now extend the results for the bi-conical pore to a sinusoidal shaped pore. Such a pore shape is interesting because it has zero slope at both the throats and the apex of the pore body. One might therefore expect that no jump in the lamella would occur, but as we show below this is not the case. Even in such a smoothly-bounded pore body, there is a significant time-averaged pressure drop due to an asymmetric jump. Rossen discusses the 3D case with a symmetric jump [12] and the 2D case with an asymmetric jump [14].

In general, there is no simple stability criterion for predicting when a jump should occur in a given 2D or 3D pore. Whereas for the bi-conical pore the jump occurred at the beginning of the rounded region, it is not usually possible to make such a prediction. We expect a *symmetric* jump when the volume, as a function of distance along the pore, goes through a maximum. However, for the asymmetric jump we must examine the eigenvalues of the Hessian of energy to make such a prediction.

In both two and three dimensions we define the boundary of the sinusoidal pore, shown in Fig. 2(ii), by

$$r_s(x) = \left(\frac{R_t + R_b}{2}\right) - \left(\frac{R_b - R_t}{2}\right)\cos\left(\frac{\pi x}{L}\right) \tag{5}$$

for $0 \leq x \leq 2L$, with parameters having the same meaning as for the bi-conical pore.

4.1 Symmetric jump

The area behind the 2D sinusoidal pore goes through a maximum when $x = 0.89L$, for which $V_D = 0.518$ (for the same parameter values as above, that is $R_t = 0.2L$ and $R_b = L = 1$). The results for the volume as a function of the positions of attachment of the film and for the pressure as a function of volume are shown in Figs. 10 and 11 respectively. In the 3D sinusoidal pore there is no maximum in $V_D(x)$ and therefore *no symmetric jump*. We find

$\Delta p_D^{\text{ave}} = 0.0103$ 2D sinusoidal pore; symmetric jump
$\Delta p_D^{\text{ave}} = 0.0000$ 3D sinusoidal pore; symmetric jump

The value for the symmetric jump in 2D is very low in comparison with that for the bi-conical pore, due to the more rounded nature of the pore shape.

4.2 Asymmetric jump

There are asymmetric jumps in both 2D and 3D, however, whose properties we explore using the Evolver. We must first ensure that we can accurately predict the point of instability, and to do this we examine the Hessian eigenvalues in a restricted 2D model.

We wish to look for the eigenvalue corresponding to the eigenmode in which one point of attachment moves forward while the other moves back. When the value of this eigenvalue shrinks to zero, the asymmetric jump is initiated. To do this in the Evolver, using the "Hessian menu" suite of commands, we first create just the opening half of the sinusoidal pore with the lamella inside. Since the only degrees of freedom which we wish to allow are those corresponding to the movement of the lamella, we must fix all other vertices (and edges) which define the pore boundary; this restricts the level of refinement that we can use, since these fixed vertices must not be close to the ends of the lamella. Then for a range of values of V_D we can find the value of the lowest eigenvalue (which does indeed correspond to the required mode). We find that it shrinks to zero at $V_D = 0.44$, and therefore predict that this should be the point of instability for the asymmetric jump.

We are currently unable to do the same in the 3D case, because of the need for a high level of refinement to accurately model the surface of the pore. It does not seem likely that, as opposed to the case of the bi-conical pore, the lamella will flip to the asymmetric shape at the same position as in 2D. Indeed, the full Evolver simulations described below find a slightly different value of both the critical position and volume.

Results from full Evolver simulations for the pressure drop across a lamella and its two points of attachment are shown for 2D and 3D in Fig. 10. The jump to the asymmetric shape occurs much earlier than in the bi-conical case, when $x \approx 0.73L$ ($V_D \approx 0.45$) in 2D, in good agreement with the prediction above, and when $x \approx 0.75L$ ($V_D \approx 0.43$) in 3D.

In 2D, in contrast to the bi-conical case, the pressure is not exactly zero during the asymmetric phase of the lamella's motion, since the walls of the pore are not parallel. However, as before, there is a larger time-averaged pressure drop in 2D compared to 3D:

$$\Delta p_D^{\text{ave}} = 0.0970 \quad \text{2D sinusoidal pore; asymmetric jump}$$
$$\Delta p_D^{\text{ave}} = 0.0716 \quad \text{3D sinusoidal pore; asymmetric jump.}$$

The values for the asymmetric jumps are roughly half the values for the respective cases in the bi-conical pore.

5 Discussion

The values of the time-averaged pressure drop in each of the cases discussed are collated in Table 1. It shows that an asymmetric jump always leads to higher time-averaged pressure drops than a symmetric jump for the same pore shape. In the bi-conical pores, as the degree of smoothing, ϵ, increases, the pressure drops all decrease; this decrease is more rapid in 3D. For instance, as ϵ increases from zero to 0.05, the pressure drop due to the symmetric jump in 2D decreases from 0.120 to 0.085, while in 3D the pressure drop associated with the symmetric jump decreases more steeply from 0.126 to 0.079. This decrease in pressure drop culminates in the very low values for the sinusoidal pore, for which there is no 3D symmetric jump, and therefore $\Delta p_D^{\text{ave}} = 0$.

As a representative calculation, consider a 3D porous medium with bi-conical pores with $\epsilon = 0.05$, a capillary entry pressure of 3000 Pa (about 1/2 psi), and bubbles 1 mm long. In this case the minimum pressure gradient for flow would be (0.104)(3000)/(0.001) or 312,000 Pa/m (about 14 psi/ft). Estimates can be much larger if the bubbles are smaller or the capillary entry pressure higher.

Liquid present in the Plateau borders plays several roles in the movement of lamellae through pores that are not accounted for here. First, if insufficient liquid is present, i.e. if capillary pressure is too high, the lamella may break, especially as it stretches across the pore body [3, 4]. We assume here that the lamella does not break.

Secondly, water occupying the corner at the pore body effectively rounds off the pore body, reflected here in the parameter ϵ. ϵ represents the distance from the pore body at which the Plateau border at the end of the lamella "senses" the water in the apex; in 3D it is related to the capillary pressure p_c as follows [9]:

$$\frac{p_c}{p_c^e} = \frac{R_t}{2L\epsilon}\left(cos(\beta) + sin(\beta)\right) \tag{6}$$

where p_c^e is the capillary entry pressure from (4) and $\beta = \tan^{-1}((R_b - R_t)/L)$, as defined in figure 2. In 2D p_c/p_c^e is twice the value in (6), because p_c^e is half as large. For the parameter values used here for the bi-conical pore, $(R_b/L = 1, \epsilon = 0.05)$, the capillary pressure p_c is about 2.8 times the capillary entry pressure of the pore. A smaller value of capillary pressure would correspond to a larger value of ϵ, and a smaller value of Δp^{ave}. The sinusoidal pore, however, gives confidence that the yield stress does not go away even for highly rounded pore geometries.

Third, if the capillary pressure is sufficiently low, bubbles may separate completely from each other in the pore throat [13]. This increases the value of Δp^{ave} [13]. Exactly what ensues depends on whether liquid in the Plateau borders is in equi-

librium with or isolated from the surroundings (or something in between), and the solution for that case is not fully worked out. Finally, if capillary pressure is sufficiently low, a process of snap-off can produce new lamellae splitting a long bubble into two [3, 12].

These effects of liquid are not accounted for here, except, implicitly, the effect of liquid occupying the corner at the pore body.

Acknowledgements

SJC wishes to thank K. Brakke for assistance with the Surface Evolver. SJC, SN, WRR and JJC acknowledge support through a grant from the Royal Society and the Royal Irish Academy. WRR acknowledges support of the U.S. Department of Energy, through contract DE-FC26-01BC15318, and a Faculty Research Assignment from The University of Texas at Austin.

References

[1] R. Gdanski, *Oil and Gas J.* **6** (1993) 85.
[2] L. L. Schramm (Ed.), *Foams: Fundamentals and Applications in the Petroleum Industry* ACS Advances in Chemistry Series No. 242, Am. Chem. Soc., Washington, D.C. (1994).
[3] W.R. Rossen, in R. K. Prud'homme and S. Khan (Eds.), Foams: Theory, Measurements and Applications, Marcel Dekker, New York, 1996.
[4] G. J. Hirasaki, R. E. Jackson, M. Jin, J. B. Lawson, J. Londergan, H. Meinardus, C. A. Miller, G. A. Pope, R. Szafranski and D. Tanzil, in S. Fiorenza, C. A. Miller, C. L. Oubre and C. H. Ward (Eds.), Surfactants, Foams, and Microemulsions, Lewis Publishers, Boca Raton 2000.
[5] R. A. Ettinger and C. J. Radke, *SPE Reservoir Eng.* **7** (1992) 83.
[6] J. V. Gillis and C. J. Radke, *Proc. 65th Annual SPE technical conference* New Orleans, LA (1990) Paper SPE 20519.
[7] F. Friedmann, W. H. Chen and P. A. Gauglitz, *SPE Reservoir Eng.* **2** (1991) 37.
[8] A. H. Falls, G. J. Hirasaki, T. W. Patzek, P. A. Gauglitz, D. D. Miller and J. Ratulowski, *SPE Reservoir Eng.* **3** (1988) 884.
[9] Q. Xu and W.R. Rossen, *Coll. Surf. A: Physicochem Eng. Aspects* **216** (2003) 175.
[10] A. H. Falls, J.J. Musters and J. Ratulowski, *SPE Reservoir Eng.* **4** (1989) 155.
[11] A. R. Kovscek, T. W. Patzek and C. J. Radke, *Chem. Eng. Sci.* **50** (1995) 3783.
[12] W.R. Rossen, *J. Coll. Interf. Sci.* **136** (1990) 1.
[13] W.R. Rossen, *Proc. SPE/DOE EOR Symp.* Tulsa, OK, April 17-20 (1988) Paper SPE 17358.

[14] W.R. Rossen, *J. Coll. Interf. Sci.* **136** (1990) 17.
[15] W.R. Rossen, *J. Coll. Interf. Sci.* **136** (1990) 38.
[16] W.R. Rossen, *J. Coll. Interf. Sci.* **136** (1990) 457.
[17] K. Brakke, *Exp. Math.* **1** (1992) 141.

Table 1
The time-averaged pressure drop for the motion of a lamella through a pore in each of the cases considered. Results followed by a reference are analytic results given by Rossen, with which the Surface Evolver results agree.

Shape	Jump	ϵ	Δp_D^{ave}
2D bi-conical pore	Symmetric	0	0.120[12]
2D bi-conical pore	Symmetric	0.05	0.0853
2D bi-conical pore	Asymmetric	0	0.217[15]
2D bi-conical pore	Asymmetric	0.05	0.178
3D bi-conical pore	Symmetric	0	0.126[12]
3D bi-conical pore	Symmetric	0.05	0.0793
3D bi-conical pore	Asymmetric	0	0.138
3D bi-conical pore	Asymmetric	0.05	0.104
2D sinusoidal pore	Symmetric	–	0.0103
2D sinusoidal pore	Asymmetric	–	0.0970
3D sinusoidal pore	Symmetric	–	0
3D sinusoidal pore	Asymmetric	–	0.0716

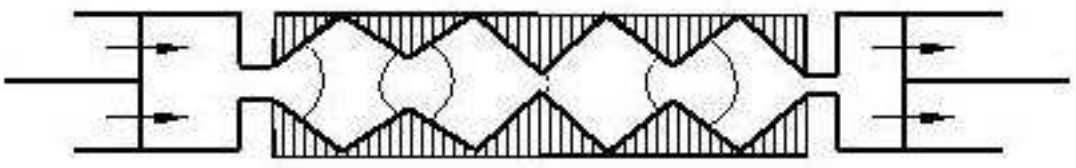

Fig. 1. Schematic of a “bubble train” moving through a porous medium. Reproduced from [9].

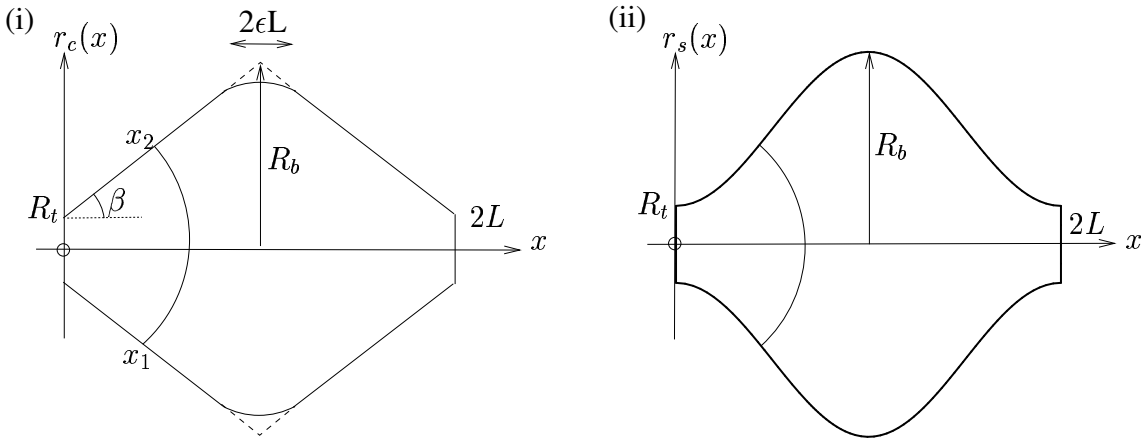

Fig. 2. Pore-geometry parameters (i) Bi-conical pore. (ii) Sinusoidal pore. Each pore is of length $2L$. The widest part of the pore body has radius R_b and the throat has radius R_t. The points of attachment of the lamella to the pore walls are denoted x_1 and x_2, which are equal when the lamella is a circular arc/spherical cap. The bi-conical pore has slope β and its apex is rounded over a length $2\epsilon L$.

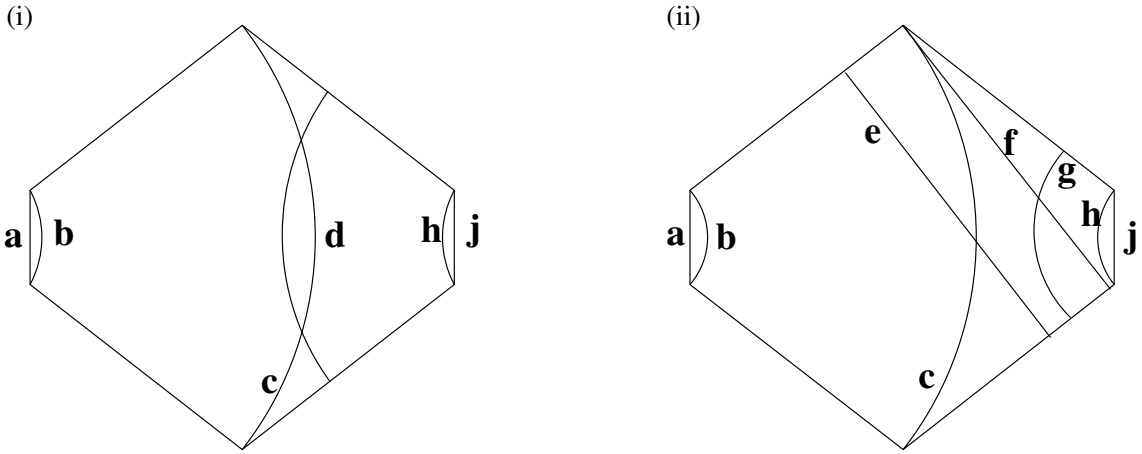

Fig. 3. Lamella shapes for the symmetric and asymmetric jumps in a 2D bi-conical pore (the rounding at the apex of the pore body is excluded). (i) In the symmetric case the lamella reaches **c** and then flips to the rearward-facing arc **d** while keeping the same volume behind it. (ii) In the asymmetric case, there is a region at the centre of the pore where the lamella is a straight line (**e** – **f**) before flipping back to the rearward-facing arc at **g**. The symmetric jump in 3D is similar, but the 3D asymmetric jump allows the lamella to assume more complicated shapes.

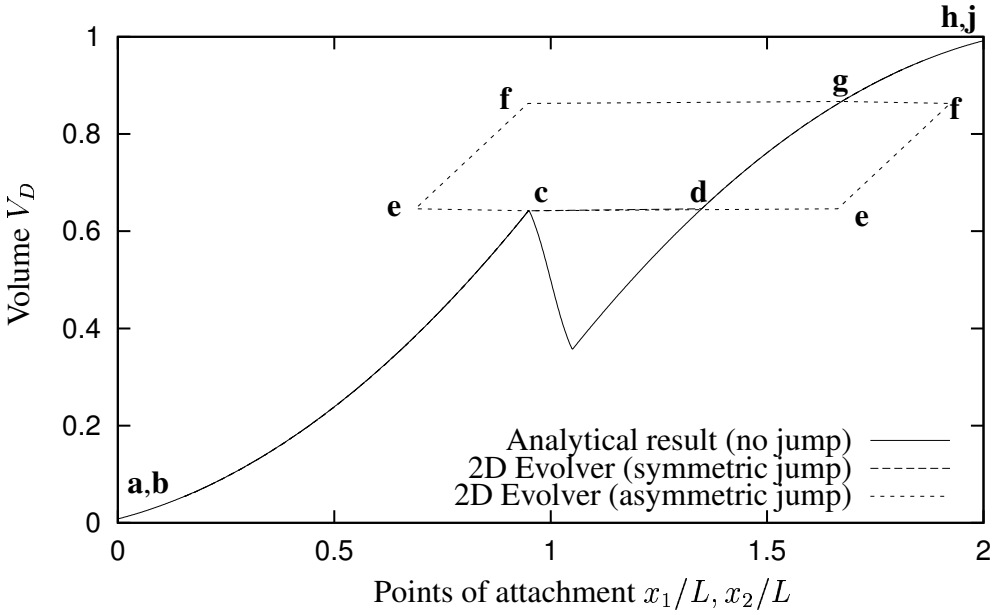

Fig. 4. The dimensionless volume (area) V_D behind a lamella in a 2D bi-conical pore with $\epsilon = 0.05$, as a function of the positions of attachment to the pore wall, x_1/L and x_2/L. The solid line beyond point **c** shows the volume if the jump were suppressed and symmetry enforced as the lamella passed through the centre of the pore; the volume decreases after reaching the rounded region at the centre of the pore. Also shown are Evolver simulations for the symmetric and asymmetric jumps. Before and after the jumps all expressions agree. The symmetric jump occurs at $x_1 = x_2 = L(1 - \epsilon)$, which is the maximum of $V_D(x)$, showing excellent agreement between the Evolver simulation and the analysis. The effect of increasing ϵ is that the jumps occur at lower x, the drop in the analytic expression for volume is reduced and smoothed, and the time-averaged pressure drop is reduced (see Fig. 5). The letters refer to the lamella shapes in Fig. 3.

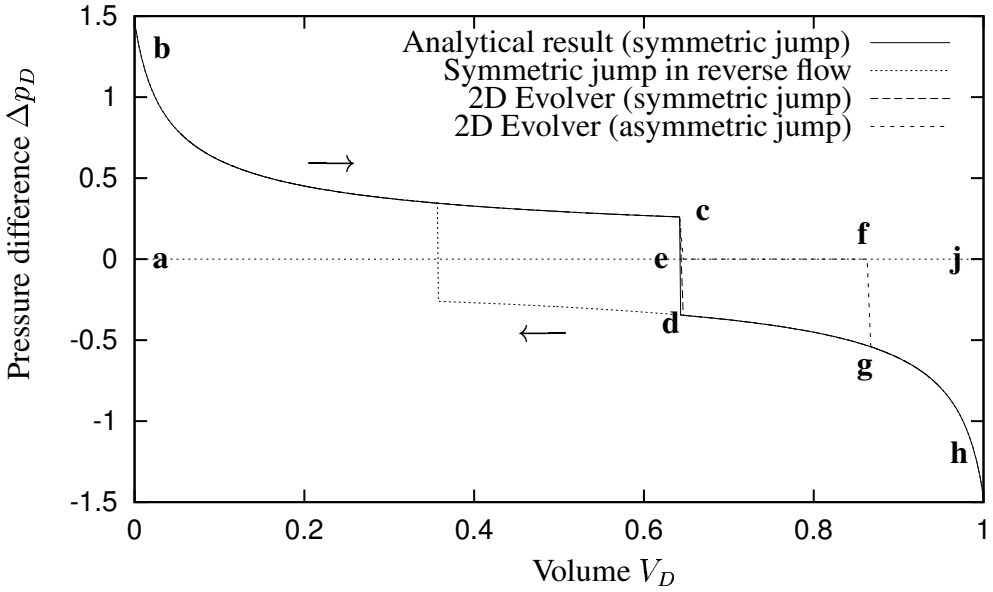

Fig. 5. The dimensionless pressure difference Δp_D across a lamella in a 2D bi-conical pore as a function of dimensionless volume (area) V_D behind the lamella. Both the symmetric and asymmetric jumps are shown for $\epsilon = 0.05$. The dotted line shows the pressure drop that would be observed in backward motion through the pore. The integral of each curve gives the time-averaged pressure drop $\Delta p_D^{\rm ave}$. This is largest for the asymmetric jump, but decreases with increasing ϵ for both symmetric and asymmetric jumps. The letters refer to the lamella shapes in Figs. 3 and 4.

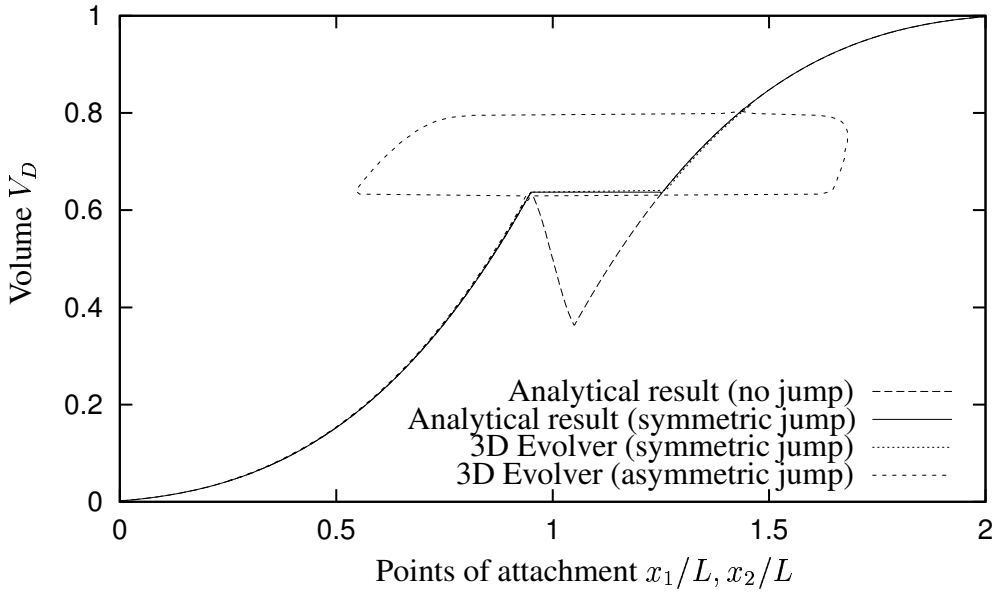

Fig. 6. The dimensionless volume V_D behind a lamella in a 3D bi-conical pore with $\epsilon = 0.05$, as a function of the maximum and minimum positions of attachment to the pore wall, x_1/L and x_2/L. As in 2D (Fig. 4) there is good agreement between simulation and theory for the symmetric jump. The asymmetric lamella shape (see Fig. 8) doesn't stretch as far toward the pore throats as in 2D but returns more quickly and more smoothly to the spherical cap.

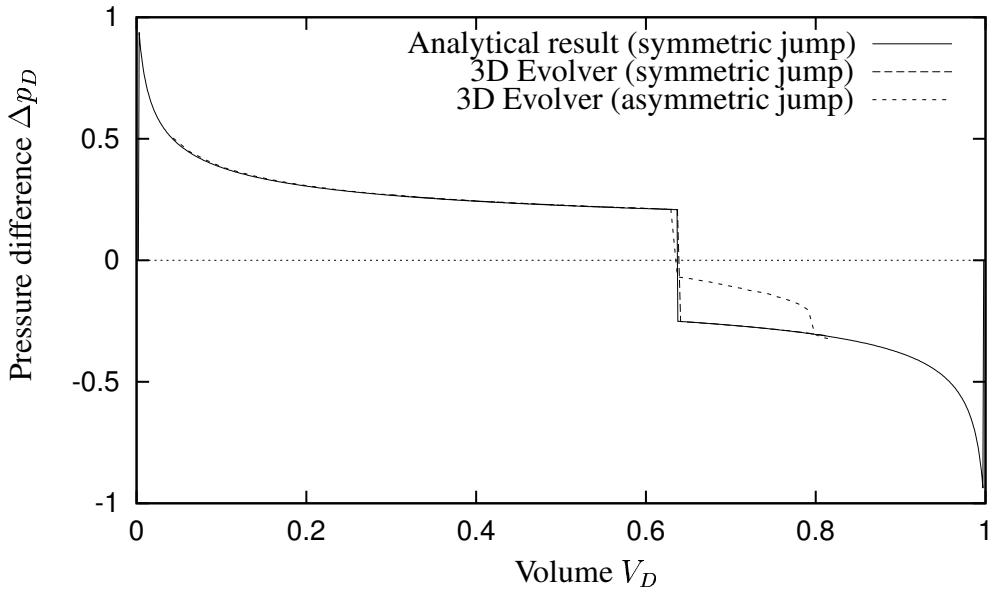

Fig. 7. The pressure difference Δp_D across a lamella in a 3D bi-conical pore as a function of dimensionless volume V_D behind the lamella. Both the symmetric and asymmetric jumps are shown for $\epsilon = 0.05$ (same data as Fig. 6). As in 2D, there is a larger time-averaged pressure drop for the asymmetric jump.

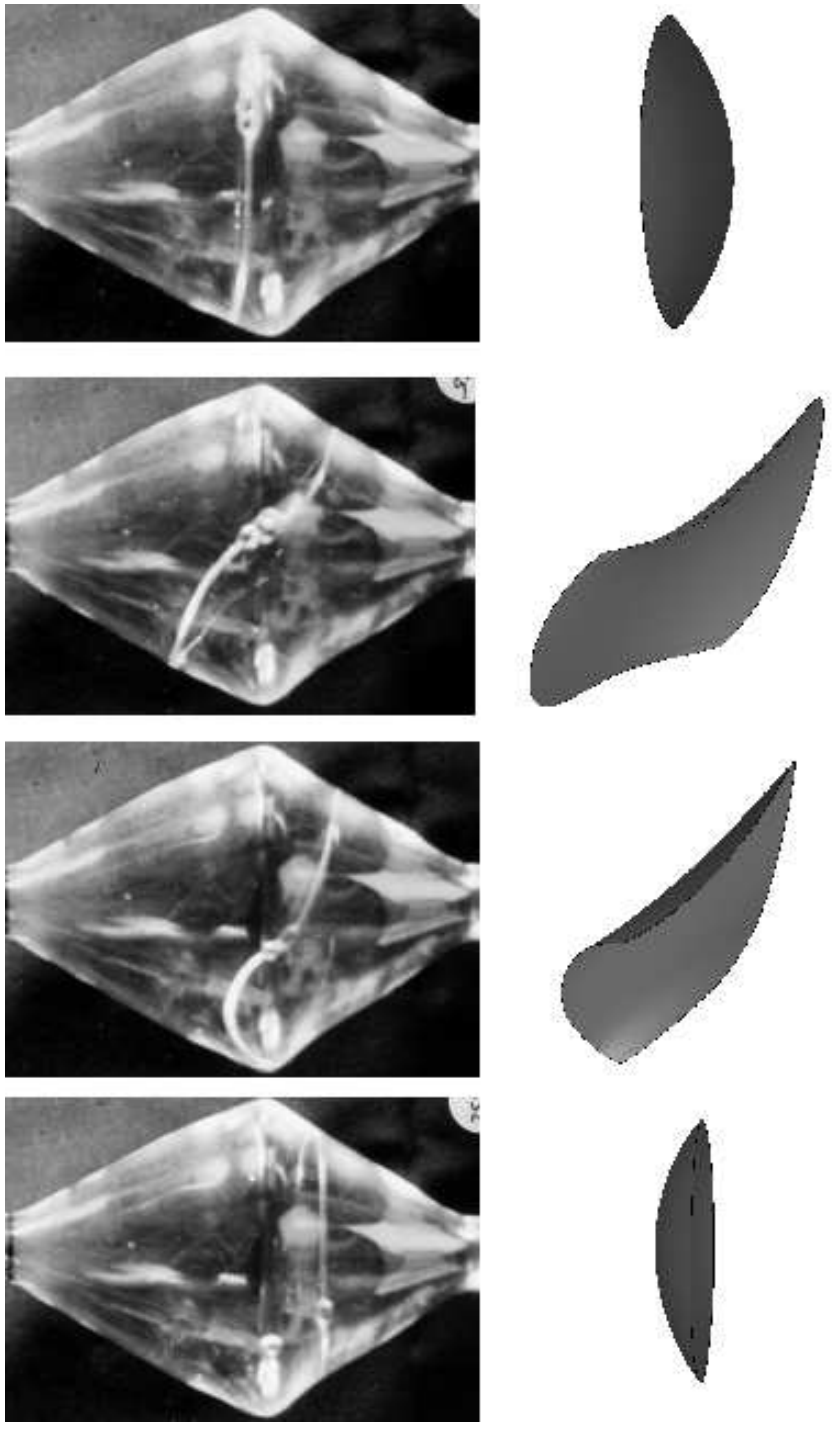

Fig. 8. Lamella shapes in 3D were obtained in experiments by Rossen [15]. Shown on the left are a series of photographs (time increases downwards) showing the asymmetric flip as the lamella is pushed through the pore from left to right. On the right we show an oblique view of the calculated shape of the lamella, for a similar bubble volume, from the Surface Evolver simulations. In the pore throats at each end, the lamella is a spherical cap, but close to the centre of the pore it flips to a saddle shape of constant mean curvature; the value of the mean curvature increases (i.e. becomes increasingly negative) as the volume of the bubble behind it increases.

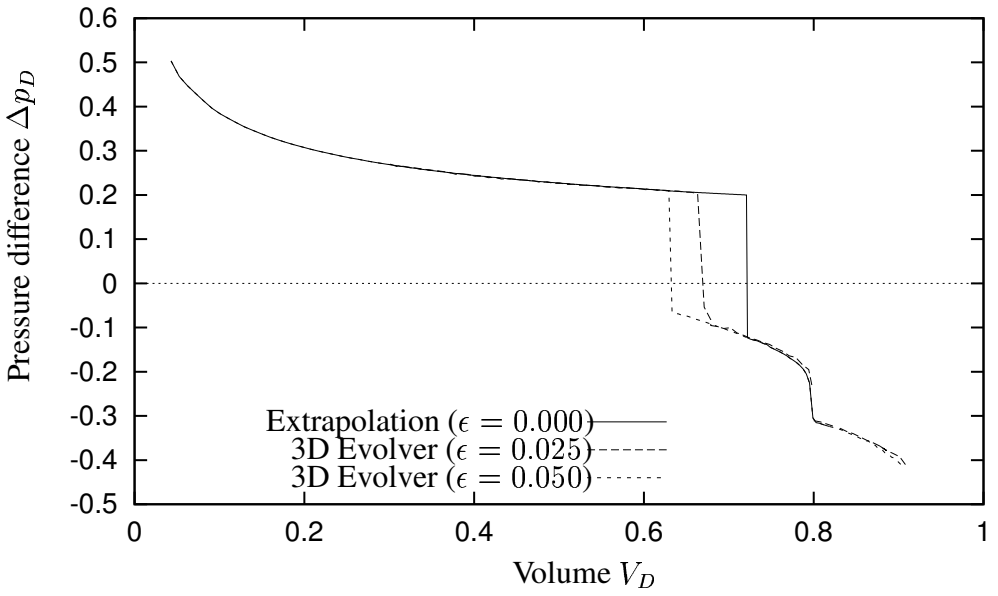

Fig. 9. The pressure difference across a lamella in a 3D bi-conical pore, as a function of the dimensionless volume V_D behind it, for different values of ϵ. The close proximity of the data from the Surface Evolver for non-zero values of ϵ shows that the pressure changes little, even for the asymmetric shapes; the only difference is the point at which the jump occurs. This allows us to infer a value for the dimensionless average pressure drop for $\epsilon = 0$.

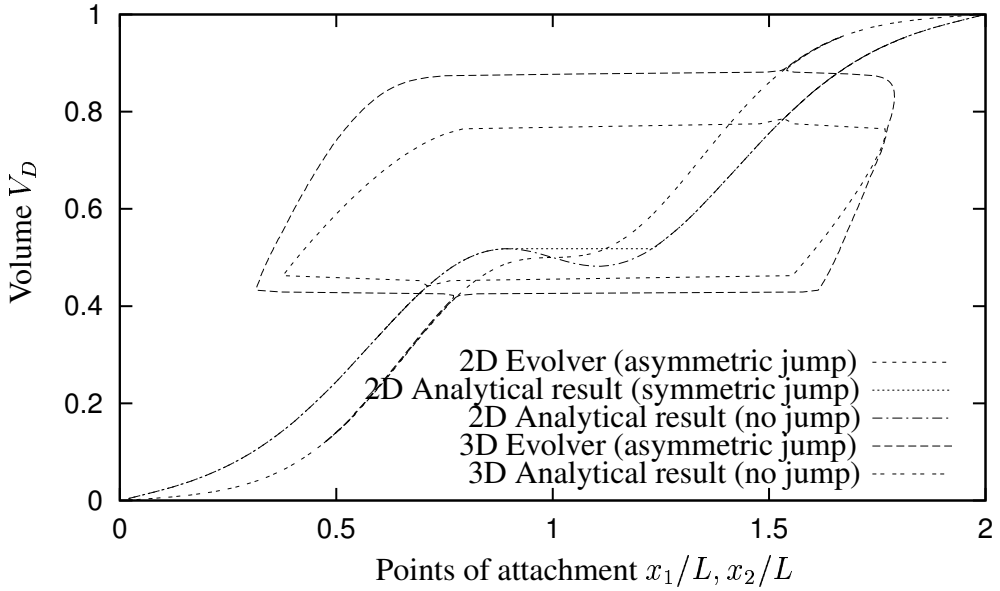

Fig. 10. The dimensionless volume V_D behind a lamella in a sinusoidal pore in 2D and 3D as a function of the maximum and minimum positions of attachment to the pore wall, x_1/L and x_2/L. In the Evolver simulations we find only the asymmetric jump, but we note that the analytic calculations show a maximum in the area behind the lamella in 2D. We therefore expect a jump in this case, with only a small average pressure drop. Both of the asymmetric jumps are similar, occurring at almost the same value of x, although in 3D the relative volume that this represents is smaller.

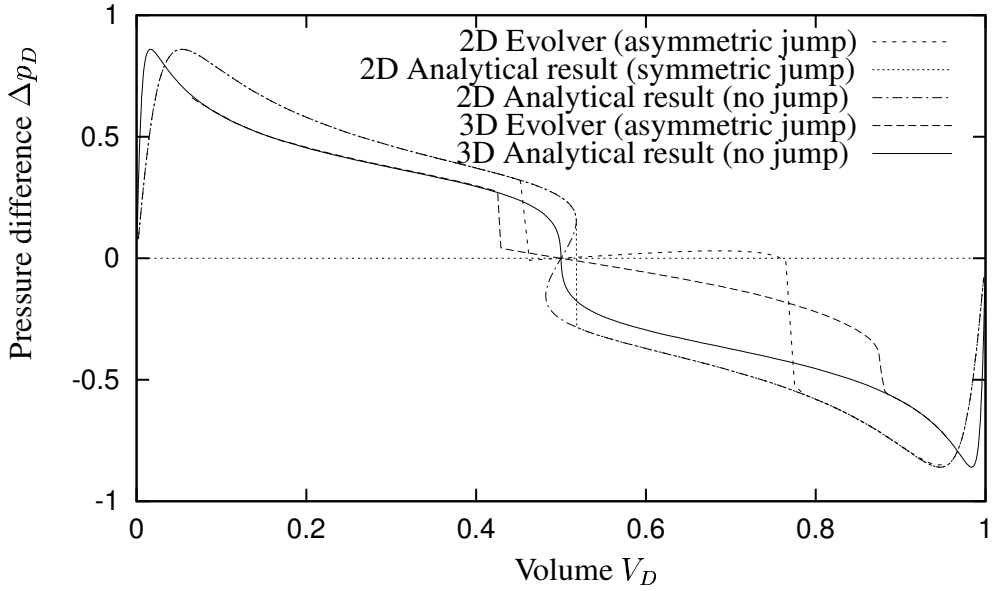

Fig. 11. The pressure difference Δp_D across a lamella in a sinusoidal pore in both 2D and 3D as a function of dimensionless volume V_D behind the lamella. In 2D the asymmetric lamella doesn't have zero pressure difference as it does in the bi-conical case. There is no symmetric jump in the 3D pore.